Clinical Cancer Research

Intraperitoneal oxidative stress in rabbits with papillomavirus-associated head and neck cancer induces tumoricidal immune response that is adoptively transferable

Annette Rossmann, Robert Mandic, Jochen Heinis, et al.

Clin Cancer Res Published OnlineFirst June 18, 2014.

Intraperitoneal oxidative stress in rabbits with papillomavirus-associated head and neck cancer induces tumoricidal immune response that is adoptively transferable

Annette Rossmann[1,2], Robert Mandic[2], Jochen Heinis[3], Helmut Höffken[3], Oliver Küssner[3], Ralf Kinscherf[4], Eberhard Weihe[1], Michael Bette[1]

[1]Department of Molecular Neuroscience, Institute of Anatomy and Cell Biology, Philipps University, Robert-Koch-Str. 8, 35037 Marburg, Germany. [2]Department of Otorhinolaryngology, Head and Neck Surgery, University Hospital Giessen and Marburg, Campus Marburg, Baldingerstr., 35033 Marburg, Germany. [3]Department of Nuclear Medicine, University Hospital Giessen and Marburg, Campus Marburg, Baldingerstr., 35033 Marburg, Germany. [4]Department of Medical Cell Biology, Institute of Anatomy and Cell Biology, Philipps University, Robert-Koch-Str. 8, 35037 Marburg

Running title: O_3/O_2-Pneumoperitoneum induced tumoricidal immunity

Keywords: Adoptive cell transfer, cancer therapy, HNSCC, immune surveillance, tumor infiltrating lymphocytes

Financial support: This research was funded in part by the Wirtschafts- und Infrastrukturbank Hessen.

Address correspondence to: Michael Bette, Department of Molecular Neuroscience, Institute of Anatomy and Cell Biology, Philipps University, Robert-Koch-Str. 8, 35037 Marburg, Germany Tel: +49-6421-2866780, Fax: +49-6421-2868965, e-mail: bette@staff.uni-marburg.de

Disclosure: No potential conflicts of interest were disclosed by the authors

Word count of the running text (including translational relevance and abstract): **4942**

Total number of figures and tables: **6**

Translational relevance

The observed regression of the rabbit auricular VX2 carcinoma, a model system for human head and neck cancer, after application of intraperitoneal oxidative stress, suggested a role of the immune system in tumor clearance. Here, we demonstrate this effect to be dependent on immune cells, since the number of tumor infiltrating lymphocytes and expression of immune relevant genes significantly rose in remitting tumor tissues. Furthermore, adoptive transfer of peripheral blood leukocytes, derived from the same animals, could induce tumor regression in untreated animals with continuously growing tumors. Since the investigated VX2 carcinoma is papillomavirus associated, studying the observed tumoricidal immune response in this model system carries great promise in identifying the mechanisms underlying the immune escape of HPV positive human head and neck cancers, thereby paving the way for new therapeutic approaches.

Abstract

Purpose: How tumors evade or suppress immune surveillance is a key question in cancer research and overcoming immune escape is a major goal for lengthening remission after cancer treatment. Here, we used the papillomavirus-associated rabbit auricular VX2 carcinoma, a model for studying human head and neck cancer, to reveal the mechanisms underlying the antitumorigenic effects of intraperitoneal oxidative stress following O_3/O_2-pneumoperitoneum (O_3/O_2-PP) treatment.

Experimental design: Solid auricular VX2 tumors were induced in immune competent adult New Zealand White rabbits. Animals were O_3/O_2-PP or sham treated followed by tumor ablation after reaching no-go criteria. $CD3^+$ tumor infiltrating lymphocytes (TILs) were evaluated by immunohistochemistry and expression levels of 84 immune response genes were measured by quantitative real time PCR. Adoptive transfer of peripheral blood leukocytes (PBLs), derived from animals with tumor regression, into control animals with progressing tumors, was implemented to functionally assess acquired tumor resistance.

Results: Auricular VX2 tumors regressing after O_3/O_2-PP treatment exhibited increased levels of $CD3^+$ TILs, enhanced expression of genes encoding receptors involved in pattern recognition, molecules required for antigen presentation and T cell activation, as well as inflammatory mediators. Adoptive cell transfer of PBLs from donor rabbits with regressing tumors to recipient rabbits with newly implanted VX2 carcinoma resulted in acquired tumor resistance of the host and tumor regression.

Conclusion: Intraperitoneal oxidative stress effectively converts the immune response against the papillomavirus-associated rabbit VX2 carcinoma from tumor permissive to tumoricidal and leads to a sustainable adoptively transferable oncolytic immune response.

Introduction

Treatment of cancer is one of the major challenges in medical care. Despite progress in surgery, radiotherapy, and chemotherapy, the prognosis for surviving aggressive cancer is often poor. Immunotherapies represent effective approaches to combat cancer by mobilizing components of the immune system for tumor destruction. For this, recombinant cytokines or monoclonal antibodies (mAbs) targeting tumor-specific antigens (TSAs), and their receptors or ligands were all found to exert anti-tumoral effects. Vaccination against TSAs is used as a therapeutic approach in the clinic (reviewed in (1)). To design novel therapeutic interventions that stimulate tumoricidal immune responses more effectively, the specific hallmarks of cancer have to be taken into account (2). Thus, solid tumors consist of relatively few neoplastic cells (cancer stem cells, CSC), and numerous distinct cell types and subtypes within the associated stroma that collectively facilitate tumor growth and progression. A recently added hallmark of tumor pathogenesis is the deregulation of cellular energetics due to genomic instability and the active immune evasion of cancer cells enabled by tumor-mediated inflammation (2), described as cancer immunoediting (3). However, tumor associated inflammation not only initiates and supports tumor development, but can also produce anti-tumorigenic immune responses leading to tumor regression. A meta-analysis of 52 human cancer studies with various tumor entities revealed that the dominance of tumor infiltrating lymphocytes (TILs), basically $CD3^+$ and $CD8^+$ T cells, is associated with significantly increased survival (4).

Recruitment of the body's immune response by precisely targeted interventions, encompassing anti-cancer vaccines (5), allogenic hematopoietic stem cell transplantation (6), and adoptive cell transfer (ACT) of *ex vivo* stimulated TILs offers new strategic avenues for cancer treatment (7). However, ACT is limited by the number of TILs present in tumor biopsies or by the lack of accessibility of surgical/bioptic material.

For head and neck squamous cell carcinomas (HNSCCs) an insufficient amount of bioptic tumor material often limits the use of cell based immunotherapies such as ACT, although immunotherapies are increasingly found to be effective in the treatment of HNSCCs (8). The auricular VX2 carcinoma-bearing New Zealand White (NZW) rabbit represents a generally accepted animal model, exhibiting similar growth features as observed in HNSCCs (9, 10). Similarly as the human papillomavirus-related HNSCCs, the VX2 tumor is associated with the Shope cottontail rabbit

papillomavirus (CRPV) (11, 12). Moreover, the sensitivity of VX2 tumors to local interleukin (IL)-2 therapies (13) qualifies this animal model as appropriate to test immunotherapeutic approaches.

We have recently shown that a strong oxidative stimulus generated by therapeutic insufflation of medical ozone/oxygen (O_3/O_2) gas mixture into the peritoneum (O_3/O_2-pneumoperitoneum, O_3/O_2-PP) at an advanced stage of VX2 tumor growth induced tumor eradication and the acquisition of tumor tolerance (14). The underlying cellular and molecular mechanisms of this high oxidative stress-induced tumoricidal immune response, however, are not known. Here, we analyzed the gene expression profile of mediators of the innate and adaptive immune system within the VX2 tumor tissue at an advanced stage of regression. We demonstrate that the O_3/O_2-PP-induced tumoricidal effect includes acquired VX2 tumor resistance which is adoptively transferable by PBLs from animals that had been cleared of the tumor after O_3/O_2-PP therapy. The data support current concepts of immune based cancer therapies.

Material and Methods

The animal experiments were approved by the regional board Giessen, Germany (V54-19c20-15(1) MR,Nr.34/2011) according to the German Animal Protection Law.

Animals

Overall, 40 adult Iffa Credo New Zealand White (NZW) rabbits (Charles River WIGA, Germany) in a BW range from 2.0 to 3.0 kg were used; 8 of them as donors of the VX2 cell suspension necessary for the induction of auricular tumors. Rabbits were kept in individual steel cages under standardized air conditioning at 20-22 °C, 50-60% humidity at a 12 h artificial day/night rhythm and had access to food and water *ad libitum*. Animals could acclimatize for at least 7 days in the hutch before the experimental procedure was started. Signs of distress, pain or cachexia - defined as weight loss above 20% - were criteria for euthanasia throughout the study.

Experimental design

The study consisted of two consecutive experimental phases. In the first phase (O_3/O_2-PP therapy, Fig. 1A), a solid auricular VX2 tumor was induced in n=20 animals. The tumor size was measured daily with a digital caliper and therapeutic intervention was started when the volume of the tumor had increased above 2,500

mm^3. As the VX2 tumors reached this starting volume, animals were assigned in alternating order to one of the two experimental groups: i) animals receiving an O_3/O_2-PP therapy (n=10) and, ii) sham treated animals receiving anesthesia and a peritoneal puncture but no gas insufflation (n=8). Animals were classified as cured when the tumor decreased to <25% of its maximal volume, or classified as incurably sick when the volume increased above 6,000 mm^3. These no-go criteria were based on our own initial observations that tumor decrease or increase to these limits resulted in tumor disappearance, or death within the following two months due to progressive growth or primary and/or secondary tumors. Once an auricular VX2 tumor had reached one of the no-go criteria it was surgically ablated and the animal was further observed for the development of possible metastases until day 90. At this time point the second experimental phase (adoptive cell transfer) started (Fig. 5A).

Tumor transplantation / therapeutic approach

VX2 tumor cells from frozen stocks were propagated by repeated *i.m.* passage within the quadriceps muscles of NZW rabbits. After 3 consecutive passages VX2 tumor cell suspensions were generated from fragmented tumor tissues and used for induction of auricular VX2 tumors as described (9). Tumor volume was measured daily and growth was allowed until the solid auricular tumor had reached a volume of >2,500 mm^3. At this stage a daily therapeutic treatment with O_3/O_2 gas mixture insufflated into the peritoneal cavity (O_3/O_2-PP) or sham treatment (puncture only) were performed as described elsewhere (14).

Surgical ablation of the tumor

Once the no-go criteria defined by the size of the VX2 tumor was reached, the animal was sedated by Robinul® (0.1 ml/kg BW, Riemser Arzneimittel AG, Germany) (*s.c.*) and anesthetized by a mixture of Rompun® (5 mg/kg BW, Bayer Vital GmbH, Germany) / Ketavet® (70 mg/kg BW, Pharmacia GmbH, Germany) (i.m.). Suprarenin® (1 mg/ml, Sanofi Aventis, Germany) was *s.c.* injected peritumoral, the auricular artery was ligated proximal to the tumor and the complete tumor removed off from the adventitia (Fig. 2B and C). The wound was subsequently bandaged under compression. Compresses were changed daily until the bleeding completely stopped. Analgesic treatment with Temgesic® (Essex Pharma, Germany) (*s.c.*) was maintained for at least two days, dependent on the stage of wound healing.

Blood parameters

Arterial blood samples from the auricular artery of the left tumor free ear were taken prior to inoculation of the VX2 tumor cell suspension (base value) and, shortly before the first and directly after the last treatment within the five day period of O_3/O_2-PP or sham treatment. For hematological investigations, an autoanalyzer (Vet abc^{TM} Animal Blood Counter, ABX Diagnostics, Germany) was carefully adjusted and validated for the analysis of rabbit blood. Data were expressed as mean values ± SEM.

PET-CT

Rabbits were anaesthetized by Robinul® plus Ketavet® as described and 0.14 mCi/kg BW radioactive labeled FDG (2-[18F]-fluoro-2-deoxy-D-glucose) diluted in 1 ml physiological saline solution was injected into the anterior vein of the ear contralateral to the tumor. A combined PET-CT analysis of the head and thorax was performed 30 min after FDG-injection using an integrated PET-CT device (Biograph 6 Truepoint PET/CT, Siemens Healthcare, Knoxville, TN). The PET-CT scans, data reconstruction, and analysis were performed according to previously described protocols (15).

Adoptive PBL transfer

Animals from experimental phase one were used as donors of PBLs at day 90 after VX2 tumor implantation. Blood from the lateral auricular vein was taken and PBLs were isolated by lysis of erythrocytes. For lysis, 3 ml of EDTA-blood was incubated at room temperature for 10 min in 90 ml of lysis buffer (1.55 M NH_4Cl, 100 mM $KHCO_3$, 10 mM EDTA), after spinning down the cell pellets were washed twice in Ca^{++}/Mg^{++}-free PBS. For each transfer $5*10^6$ cells in 1 ml of a physiological NaCl-solution were injected into the lateral auricular vein of the left ear. PBLs from i) 3 individual animals with tumor regression as a consequence of the O_3/O_2-PP therapy and, ii) 3 individual animals which exhibited progressive metastasizing tumor growth due to ineffective sham treatment were transferred into two recipients per donor. In parallel, to the adoptive transfer of PBLs, VX2 tumor was induced in the contralateral ear as described (9). Body temperature of the recipients was measured before and the first two days after cell transfer using a rectal thermometer.

RT^2 Profiler™ PCR Array

Information regarding the expression level of genes corresponding to the rabbit innate and adaptive immune system was assessed by the RT^2 Profiler™ PCR Array (PANZ-052ZA-24 for rabbit; SABiosciences, Germany) using probes of isolated total RNA from n=6 solid tumors under remission (induced by O_3/O_2-PP) and n=6 tumors under progression (unaffected by sham treatment). For each tumor sample, one 96-well RT^2 Profiler™ PCR Array plate containing 84 target genes and 5 independent housekeeping genes was used. Total RNA was isolated using the RNeasy Mini kit (Qiagen, Germany) and integrity, purity, and yield was analyzed with the Experion automated electrophoresis system (Bio-Rad Laboratories, Germany). Single strand cDNA from 0.5 µg total RNA was synthesized using the RT^2 first strand kit and real time PCR (ABI PRISM 7900HT System; Applied Biosystems, Darmstadt, Germany) was performed according to the instructions in the RT^2 Profiler™ PCR Array manual. The Ct values of each of the 84 target genes of a given plate were normalized with the average Ct values of the 5 independent housekeeping genes included on the same assay plate. Mean values of fold changes in mRNA levels derived from solid tumors under remission compared with mRNA expression levels of tumors under progression were calculated.

Immunohistochemistry and quantitative image analysis

Formalin fixated VX2 tumor tissue slices (7 µm thick) were immunostained with a mouse specific anti-CD3 antibody (Biozol, Germany, diluted 1:1,000) as described (16). To enhance the staining signals, the Tyramide Signal Amplification (TSA™) system (PerkinElmer, Germany) was used according to the manufactures protocol. Quantitative image analysis of immunostained $CD3^+$ T cells was performed using an Olympus AX70 microscope (Olympus Optical, Germany) including a SPOT RT Slider Camera (Diagnostic Instruments Inc., Seoul, Korea) and the MCID Image system (Imaging Research Inc., St. Catherines, Ontario, Canada). The border of staining intensity for positive signals was defined and the number of $CD3^+$ spots was automatically counted. Staining signals with a size of <10 pixel were excluded as false positive events. At least 10 tumor sections of each tumor, immunostained for CD3, were digitized, depending on the size of the tumor (small for tumors under remission). Data were calculated as number of $CD3^+$ T cells per square millimeter solid VX2 tumor tissue.

Statistics

In all analyses a *p* value <0.05 was considered as significant. For calculation of statistic differences in mRNA expression levels measured by the RT^2 Profiler™ PCR Array, a paired t test was performed by using the free RT² Profiler™ PCR Array Data Analysis software provided by the manufacturer (http://www.sabiosciences.com/pcrarraydataanalysis.php). In all other cases the GraphPad Prism Software 4.0 (GraphPad Software, La Jolla, CA) was used. If a given mRNA quantified by the RT^2 Profiler™ PCR Array was induced only in one experimental group, a nonparametric two-tailed Mann Whitney Test of the $\Delta\Delta$ct values was performed. The logrank test was used for comparison of progression/regression rates between both experimental groups. To synchronize the course of tumor growth, the time point when the primary tumor reached 2,500 mm^3 in size was set to day zero. The day of the final outcome was defined as the day a tumor had reached the no-go criteria for regression or progression. The unpaired two-tailed t-test with Welch's correction was used for comparison of changes in blood parameters directly before and after therapeutic intervention and for changes in the number of CD3$^+$ T cells detected within the tumor tissue.

Results

O_3/O_2-PP therapy eradicates solid VX2 tumors at a high success rate.

In the first experimental phase (O_3/O_2-PP therapy, experimental design is shown in Fig. 1A), VX2 tumor cell suspension was injected *s.c.* in 20 NZW rabbits which resulted in the development of a solid auricular VX2 tumor in 18 animals (tumor take-rate 90%) reaching a volume of 2,500 mm^3 at day 13±2 (Fig. 1B and C). At this stage, animals received either the O_3/O_2-PP therapy or underwent sham treatment. Tumor volume further increased until around day 18, independently of the treatment. Thereafter, in 7 out of 10 animals (70%) which had received O_3/O_2-PP treatment the tumor continuously decreased (Fig. 1B), whereas in 6 out of 8 sham treated animals (75%) tumor size further increased above a critical volume of 6,000 mm^3 (Fig. 1C). At this stage, tumors strongly ulcerate, which finally leads to death. Kaplan–Meier analysis revealed that the time to tumor regression (TTR) probability was significantly higher after O_3/O_2-PP therapy in comparison with sham treated animals (Fig. 1D). Accordingly, sham treatment had no impact on tumor development. The time to tumor progression (TTP) probability was significantly higher in the sham compared

with the O_3/O_2-PP treated group (Fig. 1E). Nevertheless, spontaneous remission occurred in 2 out of 8 sham treated animals (25%) albeit the period required for spontaneous tumor clearance was longer (19±2 days) in comparison with the time needed for O_3/O_2-PP-induced remission (14±2 days).

According to the typical course of HNSCC disease, all animals exhibiting progression of the primary tumor (n=3 for O_3/O_2-PP treatment and n=6 for sham treatment) demonstrated metastases in the ipsilateral lymph nodes (Fig. 2A). Nearly all animals which had cleared the primary tumor were free of lymph node metastases (n=6 for O_3/O_2-PP treatment and n=2 for sham treatment) except 1 animal from the O_3/O_2-PP group (Fig. 2A). Presence of metastases in cervical lymph nodes was diagnosed by PET-CT (Fig. 2D-I) in the living animal (Fig. 2 E-K) and by macroscopic (Fig. 2B) and histological postmortem examination (Fig. 2 L and M). In addition, within the 90 days observation period, the therapeutic effect of O_3/O_2-PP suggests protection against metastases.

O_3/O_2-PP-induced tumor clearance is associated with an increase in WBCs and TILs

To test the hypothesis that leukocytes are involved in the O_3/O_2-PP induced tumor defense, we analyzed major blood parameters before and directly after the last therapeutic intervention. The hemogram revealed a significant increase in white blood cells (WBCs) exclusively in O_3/O_2-PP treated animals (Fig. 3A), while other blood values remained within the physiological range (Supplementary Table S1). Quantitative image analysis exhibited a significant 5-fold increase in the number of $CD3^+$ T lymphocytes in the tissue of tumors which underwent remission as compared to the tissue of tumors which exhibited progression (Fig. 2B-D). This suggests that TILs are causally involved in VX2 tumor clearance.

Immune signature in tumors under O_3/O_2-PP-induced remission

A multiplex qPCR Assay representing 84 different inflammation relevant markers was used to decipher immune reactions occurring in tumors remitting after O_3/O_2-PP-treatment. The entire list of all components can be found as Supplementary Table S2.

Tumor remission is associated with enhanced transcription of immune-related genes in the respective tumor tissue, which include pattern recognition receptors (PRRs) (Fig. 4A), elements functionally involved in signal transduction cascades (Fig. 4B)

and factors known to modulate, regulate or support ongoing immune responses by different mechanisms (Fig. 4C). This could include the generation of a positive chemoattractant milieu by the enhanced expression of complement factor C3, the chemokine (C-C motif) ligands 2 and 3 and the local expression of proinflammatory cytokines, potentially boosting the immune response. Down-regulation of the local expression of cyclooxygenase 2 (COX-2), an enzyme required for producing immune-suppressive prostaglandins might contribute to an increase in local immune response.

The involvement of the adaptive immune system in O_3/O_2-PP-induced tumor defense is indicated by an enhanced expression of receptors and ligands involved in antigen presentation and induction of T cell immune responses (Fig. 4D). The MHC class I-related protein CD1d, which specifically presents lipid antigens to T cells, was expressed at about 8-fold higher levels in remitting tumors. In addition, the T cell co-receptor CD4, necessary for MHC class II-dependent antigen detection and the co-stimulatory binding couples CD80/CD28, CD86/CD28, and CD40/CD154 (CD40 ligand) were found elevated 2- to 6-fold (Fig. 4D). Thus, enhanced local antigen presentation seems to take place and might contribute to the tumoricidal immune response.

Differentiation of TILs into the T cell subpopulations T1, T2, T_{regs} and, T_H17 according to the accepted classification, revealed a role of T1 and T2 cells in tumor regression (Fig. 4E). Expression of genes encoding receptors characteristic for T1 cells and IFNγ were significantly enhanced and the expression of the T2 associated cytokines IL-4, IL-5, and IL-10 were induced only in animals with tumor remission (Fig. 4E). Although markers for T_{regs} (CCR8) and T_H17 cells (CCR6) were not significantly enhanced in tumors under remission, the transcription factor FOXP3 was significantly elevated in tumors under remission, suggesting involvement of T_{regs} and/or T_H17 cells in tumor clearance. RORC expression was slightly reduced in remitting tumor tissues and IL-17a was always absent (Fig. 4E).

O_3/O_2-PP therapy induced acquired tumor resistance that can be transferred by ACT

PBLs isolated from donor rabbits which either had been cleared of the tumor in response to the O_3/O_2-PP therapy (assumed to be “tumoricidal” PBLs), or from sham treated rabbits suffering from progressive tumor growth (assumed to be “non-

tumoricidal" PBLs), were transferred to recipient rabbits in which an auricular VX2 tumor was induced in parallel (experimental design is shown in Fig. 5A). No signs pointing to rejection such as change in body temperature (Fig. 5B) or sickness behavior were observed in the recipient rabbits. All recipients developed an auricular VX2 tumor continuously growing until day 17 *p.i.,* irrespectively of the source of PBLs transferred (Fig. 5C). In the subsequent period, 3 out of 5 animals (60%), which had received ACT of "tumoricidal" PBLs, were able to clear the tumor (Fig. 5C). In contrast, none of the animals (6/6, 100%), which received "non-tumoricidal" PBLs showed tumor clearance (Fig. 5C). The probability of tumor progression or regression significantly differed between the two recipient groups (Fig. 5D and E). This confirmed our hypothesis, that cells of the immune system are functionally involved in the tumoricidal impact of the O_3/O_2-PP therapy.

Discussion

At the time of diagnosis tumors have often developed to a macroscopically visible and clinically critical size. At this time, defense mechanisms of the body against tumor cells have failed, probably due to immune evasion of the tumor cells (17). In the worst case, tumor cells reprogram cells of the tumor microenvironment (TME) including immune cells to promote growth and vascularization of the tumor (18, 19). On the other hand, immune based therapies have proven to be powerful weapons against cancer once the immune system is reprogrammed to detect the neoplastic cells. Novel ACT treatment paradigms showing that sensitization and activation of anti-tumorigenic leukocytes derived from the patient´s own immune system can be used as a therapeutic tool for cancer treatment (7, 20).

In this study, we were able to trigger such a tumoricidal immune response after application of a repetitive highly oxidative stimulus by insufflation of a medical O_3/O_2 gas mixture into the peritoneal cavity. O_3/O_2-PP treatment led to resistance against the tumor which was transferable by ACT. In contrast to the ACT of *ex vivo* stimulated TILs however, the O_3/O_2-PP approach does not require surgical preparation of tumor cells and TILs from solid tumors, which are often difficult to obtain.

We observed that O_3/O_2-PP treatment led to a significant increase of peripheral WBCs and $CD3^+$ TILs in the VX2 tumor tissue, compared to sham treated tumors. If the increase in WBCs depends on the O_3/O_2-PP treatment alone, or might reflect the

beginning of an expansion of anti-tumorigenic leukocytes, is unknown. The increase of $CD3^+$ TILs is in accordance with clinical studies showing that high abundance of TILs in tumors is often associated with increased survival of cancer patients (4, 21-23), whereas low density of intra- and peritumoral $CD3^+$, $CD4^+$ and $CD8^+$ cells is associated with increased risk of relapse as reported for squamous cell cervical cancer (24). Apparently, TILs are major players in cancer immune surveillance by virtue of their capacity to recognize, capture, and eliminate transformed cells (25, 26).

The molecular signature of immune response genes, measured in VX2 tumors remitting after O_3/O_2-PP treatment, indicates an enhanced activation of the innate and adaptive arms of the immune system implicating a role of activated TILs.

The up-regulation of the PRRs in remitting VX2 tumors may reflect an induction or increase in the sensitivity to detect ongoing pathological changes and might be essential for triggering the tumoricidal response. Damage-associated molecular pattern molecules (DAMPs) (27, 28) such as DNA/RNA fragments, glucose or ATP released from VX2 tumor cells by itself or from cells of the TME might function as ligands for these PRRs (29). In fact, DAMPs are often critical for tumor development. For example, pathophysiologically released ATP was described as an activator of the NOD-like receptors (NLR)P3 inflammasome, which mediates the cleavage of pro-IL-1β and pro-IL-18 to biologically active cytokines or might subsequently trigger pyroptosis (30, 31). Two central components of the inflammasome (the platform protein NLRP3 and the effector protein caspase 1 (32)) were up-regulated in remitting VX2 tumors. This might imply the formation and activation of inflammasomes within the TME and might be responsible for the increase in IL-18 gene expression (33).

The signature of enhanced PRR mRNAs might indicate an anti-tumorigenic effect of TLRs, NLRs, and RIG-I-like receptors in remitting VX2 tumors, albeit protumorigenic effects of PRRs are also known (34, 35).

Activation of PRRs leads to initiation of several signal transduction pathways resulting either in the synthesis of type I interferons (IFNs), cytokines and growth factors, or in pyroptosis of the cell (36). Consistent with the observed expression of PRRs, an increase of numerous related downstream signaling molecules and transcription factors was noted in remitting VX2 tumors. These include the essential

signal molecule MyD88 which, in relationship to TLR2, TLR4, TLR6 is known to result in mitogen-activated protein kinases and/or NF-κB dependent expression of several inflammatory cytokines (36), especially the synthesis of pro-IL-1β and pro-IL-18. Surprisingly, NF-κBIA, an inactivator of NF-κB is also enhanced in remitting VX2 tumors. However, enhanced NF-κBIA seemed unable to efficiently block NF-κB-dependent gene transcription of cytokines, because TNF-α, MIP-1α and IFNγ mRNAs were still detectable at significant levels in remitting VX2 tumors. This discrepancy might be explained by the expression of NF-κB and NF-κBIA in different cell populations within the tumor tissue.

Expression of COX-2 was decreased in the VX2 tumors under O_3/O_2-PP-induced remission. As protumorigenic effects of COX-2 derived prostaglandins such as PGE2 are related to tumor growth, angiogenesis, and inhibition of apoptosis (37), the diminished COX-2 expression in remitting tumors is likely to result in a reduction of tumor permissive factors in the tumor microenvironment. In fact, blockade of COX-2 by specific inhibitors is actually used for cancer chemotherapy (38, 39) and blockade of COX-2 by the unspecific COX-inhibitor acetylsalicylic acid gains significance (40). Further, factors involved in chemoattractants namely complement factor C3, CCL2 and, CCL3 might be causally involved in the increase of TILs in remitting VX2 tumors.

The presentation of tumor antigens in combination with costimulatory signals by APCs is essential for utilization of the adaptive arm of the immune system. The observation of enhanced expression of the binding partners CD80/CD28, CD86/CD28, CD40/CD154 (CD40L), the T helper cell specific CD4, and the MHC I related receptor CD1d in remitting VX2 tumors supports our view of a decisive role of TILs in tumor defense. In this context, it is interesting to point out that the VX2 carcinoma initially developed after Shope papillomavirus-induced transformation of normal keratinocytes (12). Similarly, about 25% of HNSCC tumors or more, dependent on their anatomical site, are associated with high-risk human papillomaviruses (HPVs) in particular the type 16 (41). The papillomavirus oncoprotein E5 is implicated in MHC-class I down regulation (42, 43) and was shown to affect MHC class II maturation in IFNγ-treated keratinocytes (44). Consistent with these reports, the VX2 carcinoma was found to express E5 mRNA at high levels (data not shown). Overexpression of E5, therefore could be related to the observed

immune escape of the VX2 tumor that was overcome by immune modulatory effects of the O_3/O_2-PP treatment.

Further gene expression analysis of T cell subtype specific receptors and cytokines, points to an involvement of effector T1 and T2 cells. The exact role of T_{regs} and T_H17 cells in the VX2 tumor model remains to be unraveled in studies to come. Based on the measured FOXP3 expression levels in remitting tumors a functional involvement of these regulatory cell types seems likely, although other markers relevant for the identification of these cells types were not significantly enhanced. Both cell types, T_{regs} and T_H17, have been described to exhibit pro- as well as anti-tumorigenic effects in different types of human cancers (reviewed in (45, 46)). The combined up-regulation of IL-2, IL-10, IL-18, and IFNγ suggests that an immune response driven by T_H1 and cytotoxic T cells and NK cells might preponderate in remitting tumors. This is in line with data, showing that IL-10 in combination with IL-2 can increase the cytolytic activity of $CD8^+$ T cells (47), and in combination with IL-18 the cytolytic activity of NK cells (48).

The most likely mechanism by which O_3/O_2-PP induces the tumoricidal response seems to be related to the stimulation of immune cells in consequence of the oxidative gas insufflated into the peritoneum. This probably includes anti-tumorigenic T cells but also resident macrophages and DCs. How the highly oxidative stimulus within the peritoneal cavity reaches and affects these leukocytes within the tumor tissue is at present unclear. In principle, two starting points of the gas are conceivable (Fig. 6). On the one hand, the radical gas could act directly on circulating immune cells (49) within the peritoneal cavity, and either activate anti-tumorigenic leukocytes, or destroy immune suppressive immune cells, e.g. suppressor T cells, which until then had blocked anti-tumorigenic cells. On the other hand, oxidation of numerous biomolecules like lipoproteins can lead to the generation of ROS and LOPs (lipid oxidation products) (50) which can function as DAMPs (51) within the peritoneum, or locally after reaching the tumor via the blood stream. In fact, ROS endogenously produced in case of cellular stress have been found to function as DAMPs and are thought to be common initiators of the NLRP3 inflammasome pathway (33, 51, 52).

Unequivocal proof that immune cells are responsible for VX2 tumor eradication has been made by adoptive transfer of isolated PBLs. The ACT of PBLs derived from

O_3/O_2-PP-treated animals, which had been able to clear the primary tumor, also led to tumor clearance in host animals with a 60% success rate. We suggest, that the adaptive immune system is crucially involved in the O_3/O_2-PP induced tumor defense and that long lasting “memory” cells against the VX2 tumor must have developed. Thus, medically implemented oxidative stress by O_3/O_2-PP is suggested as a novel therapeutic approach to induce sustainable adoptively transferable oncolytic immune responses.

Acknowledgement

The authors thank Mrs. R. Peldszus and Mrs. G. Sadowski for preparation of the VX2 tumor cell suspension and G. Schemken and Dr. M. A. Juratli for their assistance during the animal experiments. We also like to thank Dr. H. Ibelgaufts for his data base “Cope with cytokines”

References

1. Kirkwood JM, Butterfield LH, Tarhini AA, Zarour H, Kalinski P, Ferrone S. Immunotherapy of cancer in 2012. CA Cancer J Clin. 2012;62:309-35.
2. Hanahan D, Weinberg RA. Hallmarks of cancer: the next generation. Cell. 2011;144:646-74.
3. Dunn GP, Bruce AT, Ikeda H, Old LJ, Schreiber RD. Cancer immunoediting: from immunosurveillance to tumor escape. Nat Immunol. 2002;3:991-8.
4. Gooden MJ, de Bock GH, Leffers N, Daemen T, Nijman HW. The prognostic influence of tumour-infiltrating lymphocytes in cancer: a systematic review with meta-analysis. Br J Cancer. 2011;105:93-103.
5. Senovilla L, Vacchelli E, Garcia P, Eggermont A, Fridman WH, Galon J, et al. Trial watch: DNA vaccines for cancer therapy. Oncoimmunology. 2013;2:e23803.
6. Jenq RR, van den Brink MR. Allogeneic haematopoietic stem cell transplantation: individualized stem cell and immune therapy of cancer. Nat Rev Cancer. 2010;10:213-21.
7. Restifo NP, Dudley ME, Rosenberg SA. Adoptive immunotherapy for cancer: harnessing the T cell response. Nat Rev Immunol. 2012;12:269-81.
8. Varilla V, Atienza J, Dasanu CA. Immune alterations and immunotherapy prospects in head and neck cancer. Expert Opin Biol Ther. 2013;13:1241-56.
9. van Es RJ, Dullens HF, van der Bilt A, Koole R, Slootweg PJ. Evaluation of the VX2 rabbit auricle carcinoma as a model for head and neck cancer in humans. J Craniomaxillofac Surg. 2000;28:300-7.
10. Dunne AA, Mandic R, Ramaswamy A, Plehn S, Schulz S, Lippert BM, et al. Lymphogenic metastatic spread of auricular VX2 carcinoma in New Zealand white rabbits. Anticancer Res. 2002;22:3273-9.
11. Shope RE, Hurst EW. Infectious Papillomatosis of Rabbits : With a Note on the Histopathology. The Journal of experimental medicine. 1933;58:607-24.

12. Georges E, Breitburd F, Jibard N, Orth G. Two Shope papillomavirus-associated VX2 carcinoma cell lines with different levels of keratinocyte differentiation and transplantability. Journal of virology. 1985;55:246-50.

13. van Es RJ, Baselmans AH, Koten JW, Van Dijk JE, Koole R, Den Otter W. Perilesional IL-2 treatment of a VX2 head-and-neck cancer model can induce a systemic anti-tumour activity. Anticancer Res. 2000;20:4163-70.

14. Schulz S, Haussler U, Mandic R, Heverhagen JT, Neubauer A, Dunne AA, et al. Treatment with ozone/oxygen-pneumoperitoneum results in complete remission of rabbit squamous cell carcinomas. International journal of cancer Journal international du cancer. 2008;122:2360-7.

15. Gratz S, Kemke B, Kaiser W, Heinis J, Behr TM, Hoffken H. Incidental non-secreting adrenal masses in cancer patients: intra-individual comparison of 18F-fluorodeoxyglucose positron emission tomography/computed tomography with computed tomography and shift magnetic resonance imaging. J Int Med Res. 2010;38:633-44.

16. Faber M, Bette M, Preuss MA, Pulmanausahakul R, Rehnelt J, Schnell MJ, et al. Overexpression of tumor necrosis factor alpha by a recombinant rabies virus attenuates replication in neurons and prevents lethal infection in mice. Journal of virology. 2005;79:15405-16.

17. Rabinovich GA, Gabrilovich D, Sotomayor EM. Immunosuppressive strategies that are mediated by tumor cells. Annu Rev Immunol. 2007;25:267-96.

18. Quail DF, Joyce JA. Microenvironmental regulation of tumor progression and metastasis. Nat Med. 2013;19:1423-37.

19. Whiteside TL. The tumor microenvironment and its role in promoting tumor growth. Oncogene. 2008;27:5904-12.

20. Gattinoni L, Powell DJ, Jr., Rosenberg SA, Restifo NP. Adoptive immunotherapy for cancer: building on success. Nat Rev Immunol. 2006;6:383-93.

21. Galon J, Costes A, Sanchez-Cabo F, Kirilovsky A, Mlecnik B, Lagorce-Pages C, et al. Type, density, and location of immune cells within human colorectal tumors predict clinical outcome. Science. 2006;313:1960-4.

22. Kong CS, Narasimhan B, Cao H, Kwok S, Erickson JP, Koong A, et al. The relationship between human papillomavirus status and other molecular prognostic markers in head and neck squamous cell carcinomas. Int J Radiat Oncol Biol Phys. 2009;74:553-61.

23. Shibuya TY, Nugyen N, McLaren CE, Li KT, Wei WZ, Kim S, et al. Clinical significance of poor CD3 response in head and neck cancer. Clin Cancer Res. 2002;8:745-51.

24. Nedergaard BS, Ladekarl M, Thomsen HF, Nyengaard JR, Nielsen K. Low density of CD3+, CD4+ and CD8+ cells is associated with increased risk of relapse in squamous cell cervical cancer. Br J Cancer. 2007;97:1135-8.

25. Kim R, Emi M, Tanabe K. Cancer immunoediting from immune surveillance to immune escape. Immunology. 2007;121:1-14.

26. Lanca T, Silva-Santos B. The split nature of tumor-infiltrating leukocytes: Implications for cancer surveillance and immunotherapy. Oncoimmunology. 2012;1:717-25.

27. Escamilla-Tilch M, Filio-Rodriguez G, Garcia-Rocha R, Mancilla-Herrera I, Mitchison NA, Ruiz-Pacheco JA, et al. The interplay between pathogen-associated and danger-associated molecular patterns: an inflammatory code in cancer? Immunol Cell Biol. 2013;91:601-10.

28. Sansonetti PJ. The innate signaling of dangers and the dangers of innate signaling. Nat Immunol. 2006;7:1237-42.

29. Hedayat M, Takeda K, Rezaei N. Prophylactic and therapeutic implications of toll-like receptor ligands. Med Res Rev. 2012;32:294-325.

30. Zitvogel L, Kepp O, Galluzzi L, Kroemer G. Inflammasomes in carcinogenesis and anticancer immune responses. Nat Immunol. 2012;13:343-51.

31. Miao EA, Rajan JV, Aderem A. Caspase-1-induced pyroptotic cell death. Immunological reviews. 2011;243:206-14.

32. Martinon F, Petrilli V, Mayor A, Tardivel A, Tschopp J. Gout-associated uric acid crystals activate the NALP3 inflammasome. Nature. 2006;440:237-41.

33. Tschopp J, Schroder K. NLRP3 inflammasome activation: The convergence of multiple signalling pathways on ROS production? Nat Rev Immunol. 2010;10:210-5.

34. Chen R, Alvero AB, Silasi DA, Steffensen KD, Mor G. Cancers take their Toll--the function and regulation of Toll-like receptors in cancer cells. Oncogene. 2008;27:225-33.

35. Pradere JP, Dapito DH, Schwabe RF. The Yin and Yang of Toll-like receptors in cancer. Oncogene. 2013;DOI:10.1038/onc.2013.302.

36. Takeuchi O, Akira S. Pattern recognition receptors and inflammation. Cell. 2010;140:805-20.

37. Dannenberg AJ, Altorki NK, Boyle JO, Dang C, Howe LR, Weksler BB, et al. Cyclo-oxygenase 2: a pharmacological target for the prevention of cancer. Lancet Oncol. 2001;2:544-51.

38. Ghosh N, Chaki R, Mandal V, Mandal SC. COX-2 as a target for cancer chemotherapy. Pharmacol Rep. 2010;62:233-44.

39. Meric JB, Rottey S, Olaussen K, Soria JC, Khayat D, Rixe O, et al. Cyclooxygenase-2 as a target for anticancer drug development. Crit Rev Oncol Hematol. 2006;59:51-64.

40. Cook NR, Lee IM, Zhang SM, Moorthy MV, Buring JE. Alternate-day, low-dose aspirin and cancer risk: long-term observational follow-up of a randomized trial. Ann Intern Med. 2013;159:77-85.

41. D'Souza G, Kreimer AR, Viscidi R, Pawlita M, Fakhry C, Koch WM, et al. Case-control study of human papillomavirus and oropharyngeal cancer. The New England journal of medicine. 2007;356:1944-56.

42. Campo MS, Graham SV, Cortese MS, Ashrafi GH, Araibi EH, Dornan ES, et al. HPV-16 E5 down-regulates expression of surface HLA class I and reduces recognition by CD8 T cells. Virology. 2010;407:137-42.

43. Marchetti B, Ashrafi GH, Dornan ES, Araibi EH, Ellis SA, Campo MS. The E5 protein of BPV-4 interacts with the heavy chain of MHC class I and irreversibly retains the MHC complex in the Golgi apparatus. Oncogene. 2006;25:2254-63.

44. Zhang B, Li P, Wang E, Brahmi Z, Dunn KW, Blum JS, et al. The E5 protein of human papillomavirus type 16 perturbs MHC class II antigen maturation in human foreskin keratinocytes treated with interferon-gamma. Virology. 2003;310:100-8.

45. Dennis KL, Blatner NR, Gounari F, Khazaie K. Current status of interleukin-10 and regulatory T-cells in cancer. Curr Opin Oncol. 2013;25:637-45.

46. Ye J, Livergood RS, Peng G. The role and regulation of human Th17 cells in tumor immunity. Am J Pathol. 2013;182:10-20.

47. Chen WF, Zlotnik A. IL-10: a novel cytotoxic T cell differentiation factor. J Immunol. 1991;147:528-34.

48. Cai G, Kastelein RA, Hunter CA. IL-10 enhances NK cell proliferation, cytotoxicity and production of IFN-gamma when combined with IL-18. Eur J Immunol. 1999;29:2658-65.

49. Larini A, Bocci V. Effects of ozone on isolated peripheral blood mononuclear cells. Toxicol In Vitro. 2005;19:55-61.

50. Bocci VA. Scientific and medical aspects of ozone therapy. State of the art. Arch Med Res. 2006;37:425-35.

51. Zhou R, Yazdi AS, Menu P, Tschopp J. A role for mitochondria in NLRP3 inflammasome activation. Nature. 2011;469:221-5.

52. Cruz CM, Rinna A, Forman HJ, Ventura AL, Persechini PM, Ojcius DM. ATP activates a reactive oxygen species-dependent oxidative stress response and secretion of proinflammatory cytokines in macrophages. J Biol Chem. 2007;282:2871-9.

Figures

Figure 1. Experimental design and growth kinetics of VX2 tumors. A, treatment scheme of the O_3/O_2-PP therapy and the defined no-go criteria. B, C, growth kinetics of VX2 tumors in animals of the O_3/O_2-PP and sham group. Mean values ± SEM are shown if the number of samples was >3 (filled icons). If the number was ≤3 the moving average over three days is shown by dashed lines. The gray dashed line indicates the threshold of tumor volume at which the therapeutic approach started. D, Kaplan-Meier analysis depicting the time to tumor regression (TTR) probability and (E) the time to tumor progression (TTP) probability of solid auricular VX2 tumors. Treatment of each individual animal started when the auricular VX2 tumor exceeded a volume of 2,500 mm^3 and was set to day 0. The TTP or TTR probabilities were defined by the tumor volume. The TTP was reached when the tumor volume increased above 6,000 mm^3 and TTR was reached when the tumor volume decreased below 25% of its maximal volume. Statistically significant changes between the O_3/O_2-PP and the sham group were calculated by the logrank test and marked with $p<0.05^*$; numbers and percentages of tumors showing regression (B, D) or progression (C, E) are shown in brackets.

Figure 2. Metastatic spread of VX2 tumors in the rabbit. A, frequency of lymph node metastasis in animals with regressing and animals with progressing tumors. The number of animals for each therapeutic outcome and treatment is shown in brackets. Macroscopic views of (B) a submandibular sentinel lymph node harboring metastatic tumor tissue, (C) a primary auricular tumor and, (D) an ear directly after surgical ablation of the tumor. E-G, PET-CT analyses of a sham treated rabbit suffering from regional metastases at the proximal region of the ear, and the respective sentinel lymph node. H-K, PET-CT analysis of an O_3/O_2-PP-treated and tumor free rabbit. PET-CT images were 3D reconstructed and labeling intensity of [^{18}F]-FDG was depicted by false colors. The dotted lines in (F) and (I) specify the level of the frontal scan reconstructions shown in (G) and (K), respectively. Note the light areas in panels E and H marked by arrows, representing the remaining thin tissue area after tumor ablation as shown in D, exemplarily. L, M, microscopic views of a Haematoxilin/Eosin stained sentinel lymph node containing VX2 tumor metastases.

Figure 3. Effect of O_3/O_2-PP treatment on leukocyte numbers. A, changes in the number of white blood cells (WBCs) directly before the first and after the last therapeutic intervention or sham treatment. B, numbers of $CD3^+$ T cells within tumor tissues under remission or progression measured by digital image analysis of auricular VX2 tumors immunostained for CD3. Statistical differences were calculated by the two-tailed t-test with Welsh correction and marked with: *p<0.05, ***p<0.0001. Depicted are mean values ± SEM. Representative CD3-immunostained tumor sections from a VX2 tumor under remission or under progression are shown in (C) and (D), respectively. The inserts show $CD3^+$ cells present in (C) and (D) at higher magnification.

Figure 4. Expression levels of immune relevant genes in the tumor tissue. Immunologically relevant factors were grouped according to their mode of action in (A) pattern recognition receptors, (B) signal transduction factors, (C) mediators or regulators of inflammatory responses, (D) molecules functionally involved in antigen presentation to T cells and T cell activation by essential co-stimulatory signals and, (E) T cell subpopulations identified by their specific expression pattern. Shown are mean values of fold changes in mRNA levels from solid tumors under remission (induced by O_3/O_2-PP, n=6) compared with mRNA expression levels of tumors under progression (unaffected by sham treatment, n=6). Values above 0.0 represent increased expression levels in the remitting tumor. Significant differences between tumors under regression and progression were calculated with the unpaired *t*-test and marked as: *p<0.05; **p<0.01; ***p<0.001; n.s. not significant, n.d. not detected. If a given factor was induced in one experimental group only, a scatter plot of $\Delta\Delta$ct values is depicted on the right side of the equivalent bar graphs. Grey areas in each scatter plot represent the range that was defined as negative (mRNA expression not verifiable due to a ct value >35 cycles = $\Delta\Delta$ct < 0.00047). In this case a nonparametric two-tailed Mann Whitney test of the $\Delta\Delta$ct values was used. Abbreviations in bars below the x-axes: TLR: Toll-like receptors; RLR: RIG-I-like receptors; NLR: NOD-like receptors; trans.f.: transcription factor; sup.: immune suppressive, chem.at.: chemoattractant; pro.inf.: pro-inflammatory; AP: antigen presentation; IgS: Immune globulin superfamily; TNFR: tumor necrosis factor receptor superfamily; T1, T2, T17: type 1, 2, 17 T cell; T_{regs}: regulatory T cell.
Abbreviations of genes: C3: complement component 3; CCL2, 3: chemokine (C-C motif) ligand 2, 3; CCR4, 5, 6, 8: chemokine (C-C motif) receptor 4, 5, 6-like, 8;

CD1d, 4, 28, 40, 86, 154: cluster of differentiation CD1d, 4, 28, 40, 86, 154; C-Jun: C-jun transcription factor; COX-2: cyclooxygenase-2; CXCR3, 4: chemokine (C-X-C motif) receptor 3, 4; FOXP3: forkhead box P3; IFNγ: interferon gamma; IL-2, -4, -5, -13, -15, -17a, -18: interleukin-2, -4, -5-like, -13, -15, -17a, -18; IRAK1: interleukin 1 receptor-associated kinase 1-like; IRF1: interferon regulatory factor 1; MAPK1, 3, 8, 14: mitogen-activated protein kinase 1-like, 3-like, 8, 14; MDA-5: melanoma differentiation-associated gene 5; MyD88: myeloid differentiation primary response gene 88-like; NF-κB: nuclear factor kappa-light-chain-enhancer of activated B cells 2; NF-κBIA: nuclear factor kappa-light-chain-enhancer of activated B cells inhibitor alpha; NLRP3: NLR family, pyrin domain containing 3; NOD1, 2: nucleotide-binding oligomerization domain containing 1, 2; RIG-1: retinoic acid inducible gene-I; STAT1: signal transducer and activator of transcription 1; TLR1, 2, 3, 4, 6: toll-like receptor 1-like, 2, 3, 4, 6; TNF: tumor necrosis factor; TRAF6: TNF receptor-associated factor 6; TYK2: tyrosine kinase 2-like

Figure 5. Tumor resistance induced by ACT of PBLs. A, experimental design of the ACT. O_3/O_2-PP treated rabbits which have been able to clear the tumor or sham treated, tumor sick rabbits, both derived from experimental phase 1, were used as donor animals for PBL transfer. B, mean body temperature ± SEM of recipient animals before and after ACT. The physiological range of body temperature of NZW rabbits is marked in gray. C, VX2 tumor size development after simultaneous VX2 tumor cell inoculation and ACT of PBLs derived from either O_3/O_2-PP treated, cured or sham treated (tumor sick) animals. Shown are the mean values ± SEM of the VX2 tumor size from all progressively growing tumors within the PBL- sham group and from remitting tumors of the PBL-O_3/O_2-PP group. The dashed line represents the moving average over three days of progressively growing tumors of the PBL-O_3/O_2-PP group. D, Kaplan-Meier analysis of the time to tumor regression (TTR) probability and (E) the time to tumor progression (TTP) probability of solid auricular VX2 tumors. Statistically significant changes between the two groups were calculated by the logrank test and marked with $p<0.05^*$; numbers and percentages of tumors that had reached the defined tumor volume characteristic for progression or regression are shown in brackets. Mean values ± SEM are shown.

Figure 6. Proposed model for the underlying mechanisms of the O_3/O_2-PP mediated tumoricidal immune response. Within the peritoneal cavity O_3/O_2 might i.) kill immune cells including T suppressor cells, which so far have inhibited a tumoricidal immune response or, ii.) stimulate immune cells directly (direct pathway) or via the generation of ROS and LOPs (indirect pathway). Circulation of activated immune cells and ROS and LOPs via the blood stream leads to a complex immune response within the tumor tissue under joint contribution of the innate and adaptive immune system.

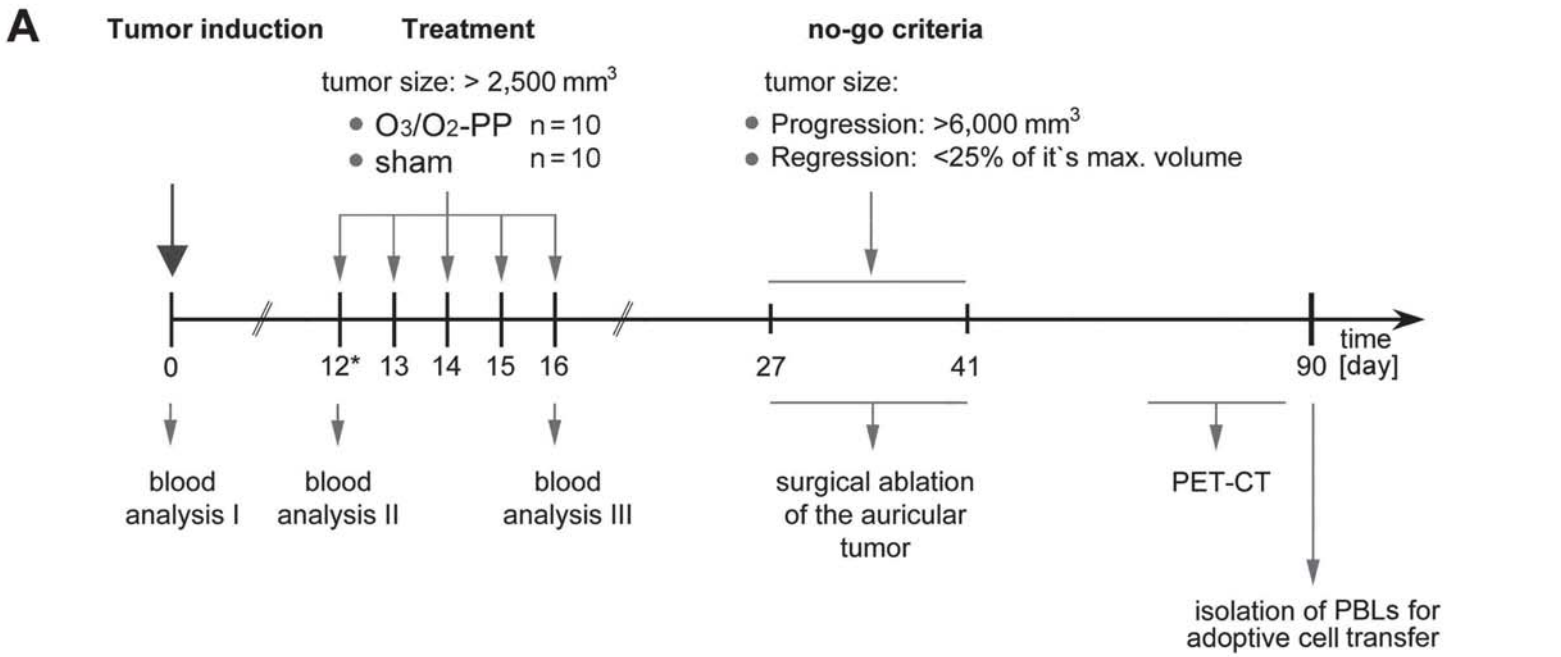

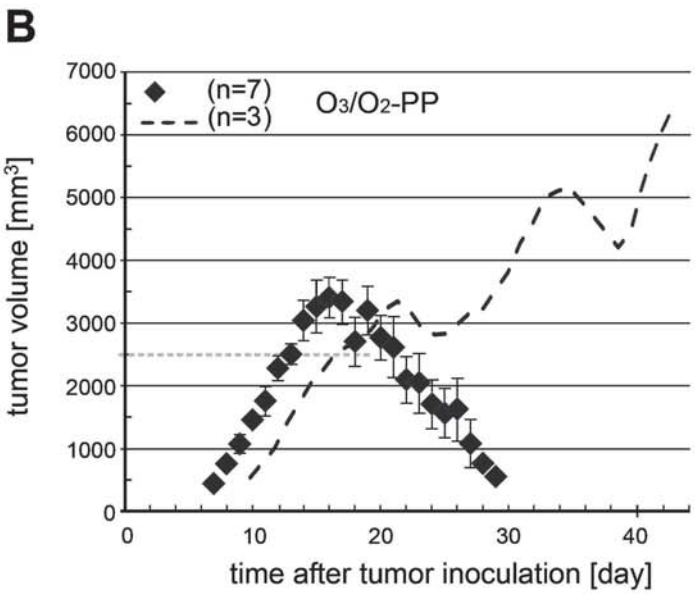

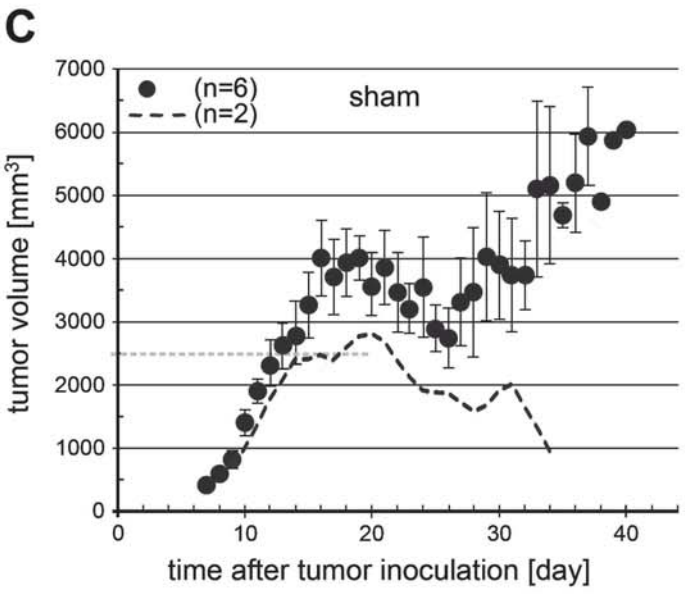

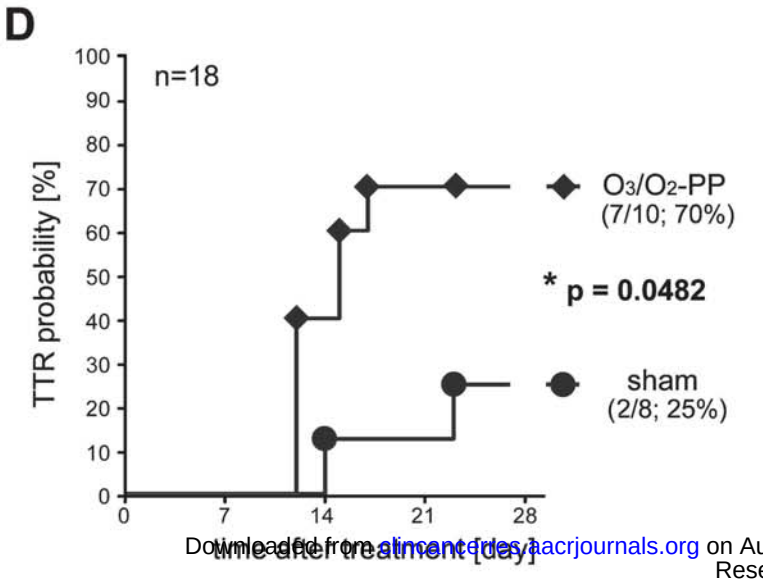

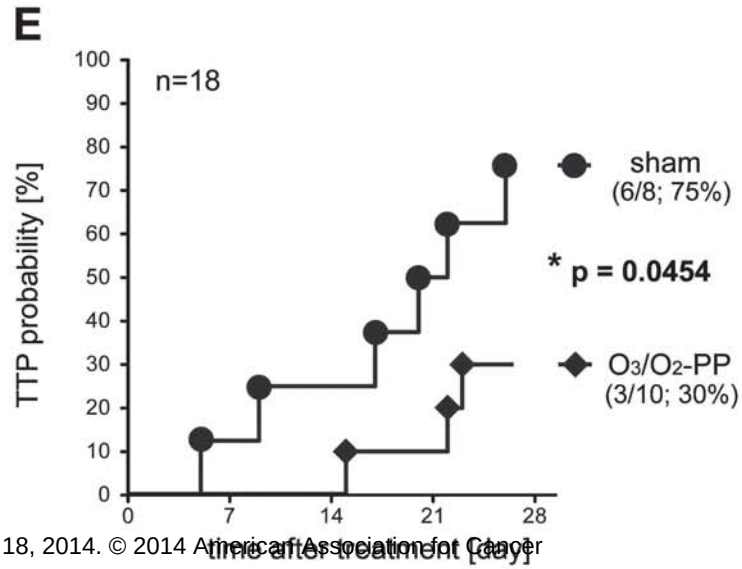

Figure 2 CCR-14-0677

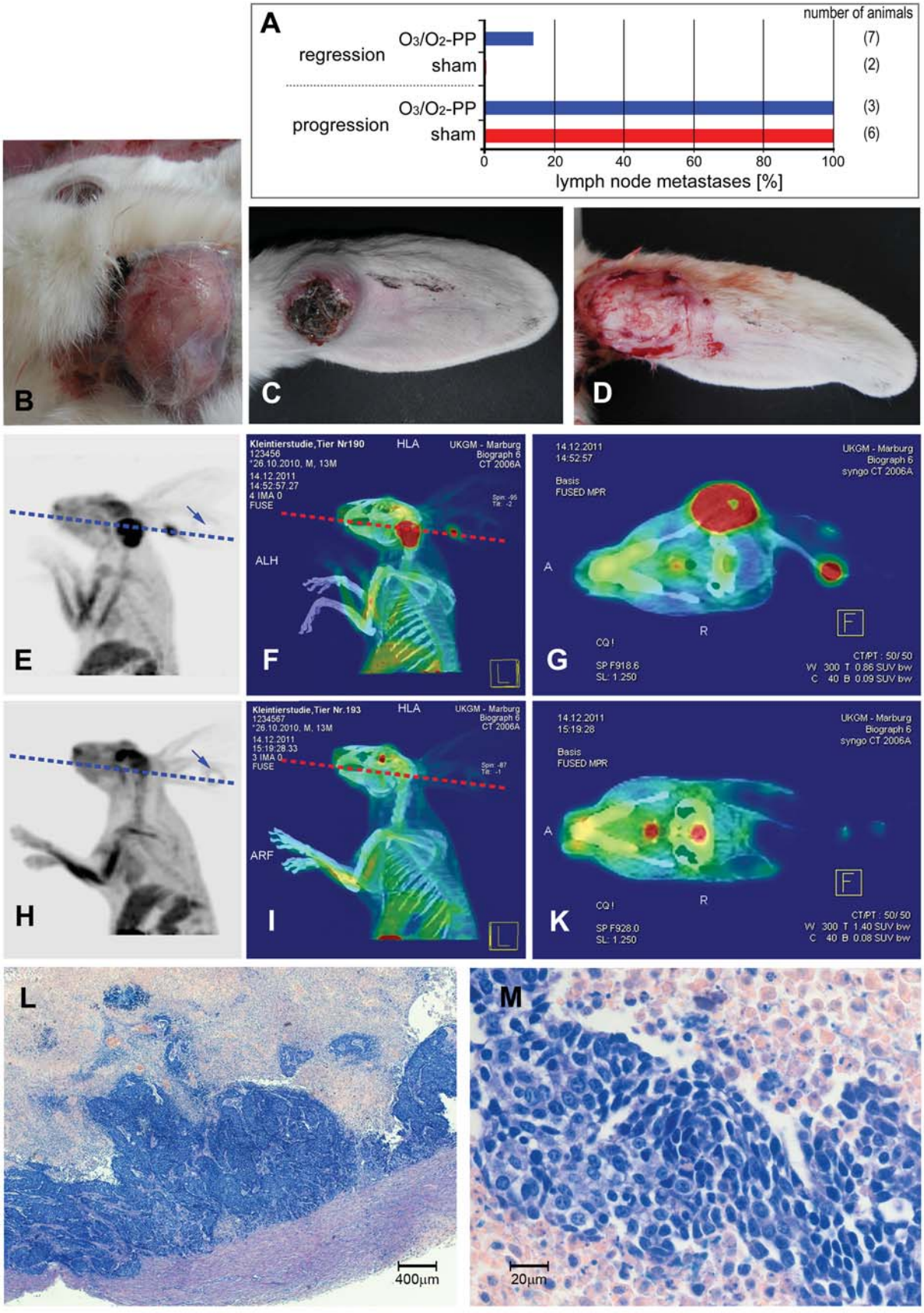

Figure 3

CCR-14-0677

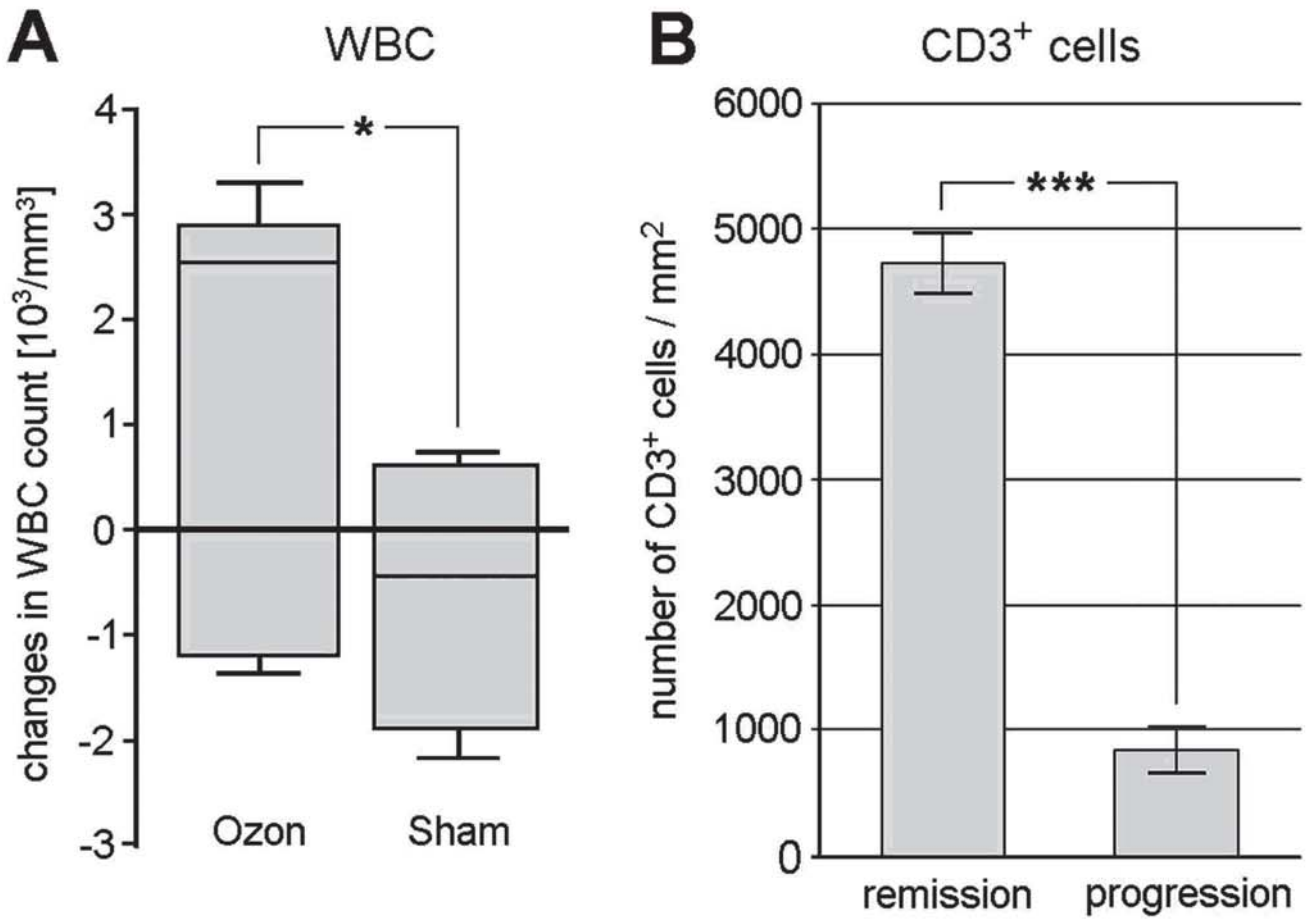

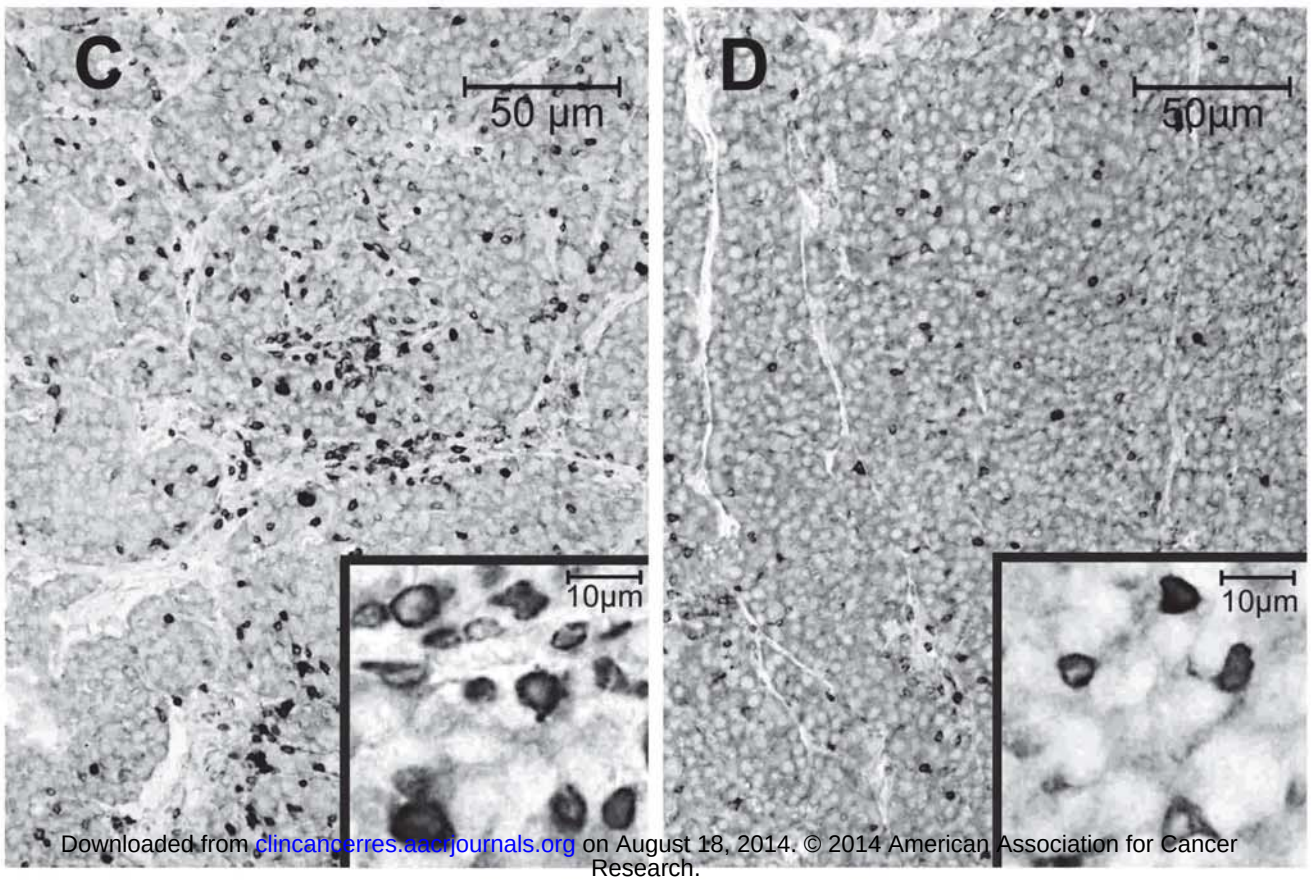

Figure 4 CCR-14-0677

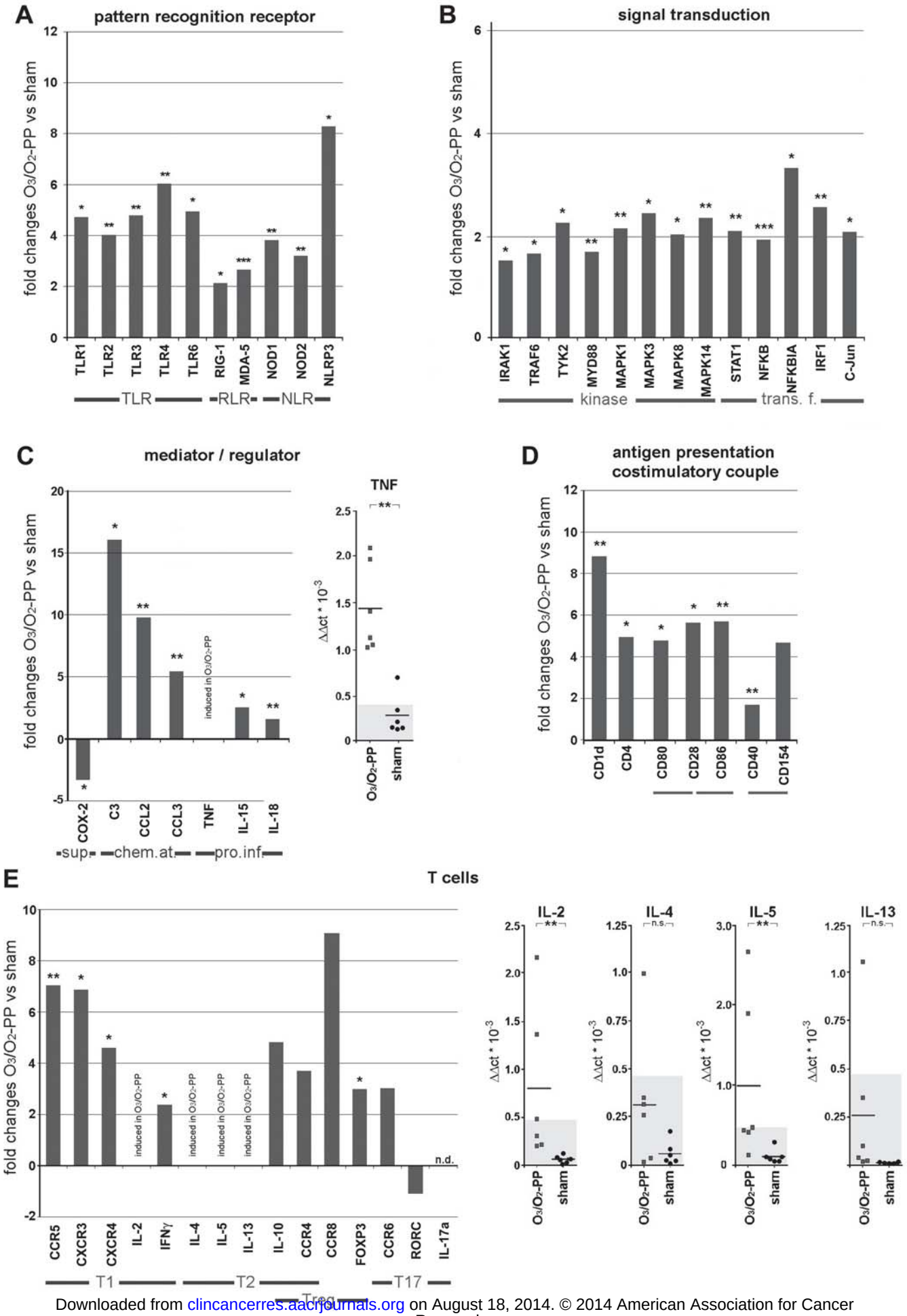

Figure 5 CCR-14-0677

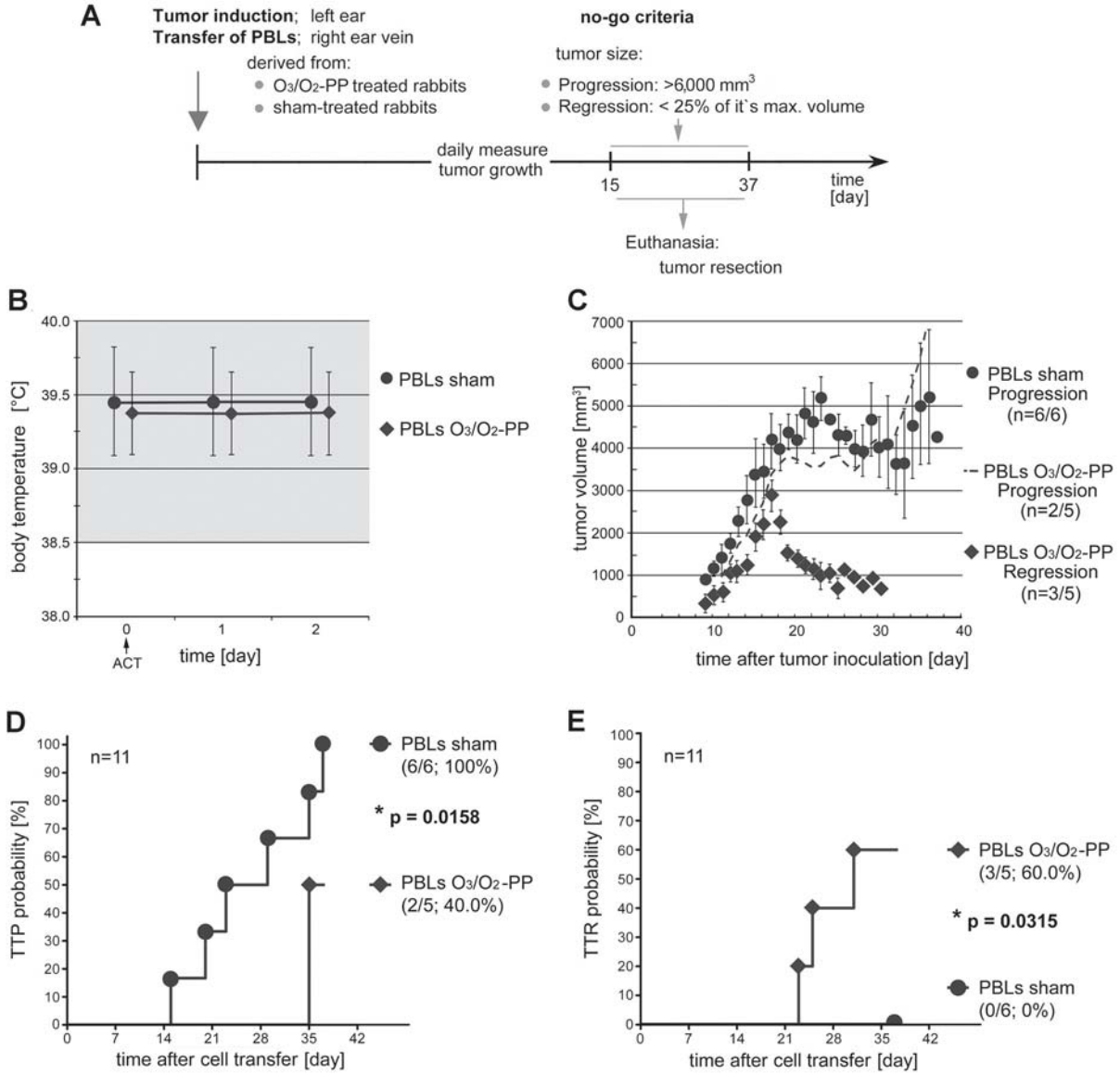

Figure 6 CCR-14-0677